The Effect of Ion Beam Surface Modifications on Fatigue Crack Initiation in Polycrystalline Nickel*

D. J. MORRISON and J. W. JONES

Department of Materials Science and Engineering, University of Michigan, Ann Arbor, MI 48109 (U.S.A.)

D. E. ALEXANDER, C. KOVACH and G. S. WAS

Department of Nuclear Engineering, University of Michigan, Ann Arbor, MI 48109 (U.S.A.)

(Received September 16, 1988)

Abstract

Flexural fatigue tests at surface strain amplitudes of ±0.0012 were conducted on polycrystalline nickel to determine the effect of ion beam surface modifications of the Ni/Al system on fatigue crack initiation. An Ni–75at.%Al surface region 1000 Å thick was produced by evaporating alternate layers of nickel and aluminum followed by ion beam mixing with 3 MeV Ni^{2+} ions to a fluence of 1×10^{16} ions cm^{-2}. A two-phase γ–γ' surface structure was produced through implantation of 350 keV Al^{+} ions to a fluence of 5×10^{17} ions cm^{-2} into the nickel specimens at 723 K. Nickel specimens that were self-implanted with 350 keV Ni^{+} ions to a fluence of 1×10^{16} ions cm^{-2} were also analyzed.

The addition of aluminum to the surface resulted in an increase in surface hardness and suppression of surface slip band features. The nickel self-implantation increased surface hardness but had very little effect on surface slip feature suppression. Transgranular crack initiation was seen in unmodified and self-implanted specimens, and intergranular crack initiation was prevalent in aluminum micro-alloyed specimens.

1. Introduction

During low-cycle fatigue of f.c.c. metals such as nickel and copper, regions of localized strain are formed. These regions have been termed persistent slip bands (PSBs) [1] due to the fact that when the bands are removed from the surface by electropolishing, subsequent cycling results in the slip bands reforming at the same places. Intrusions and extrusions form where PSBs intersect the surface and act as initiation sites for fatigue cracks [1, 2]. Since this localization of plastic strain exerts a deleterious effect on fatigue resistance, a reduction in the amount of plastic strain at the surface or a homogenization of the surface plastic strain would be expected to impede the accumulation of surface fatigue damage.

Ion beam surface modification has been shown to be an effective technique to produce "micro-alloyed" surfaces that possess properties that enhance the fatigue resistance of metals. A brief summary of research that has been conducted on the fatigue response of ion-beam-modified metals can be found in ref. 3. In most of these studies, the mechanisms cited for improving fatigue resistance were strain homogenization and increased slip reversibility produced by reducing the stacking fault energy of the surface [4, 5]; reducing surface plastic strain by increasing the yield strength of the surface layer [6, 7]; and the formation of compressive residual stresses on the surface [6].

The objective of the present work was to determine the effects that ion microalloys of the Ni/Al system have on fatigue crack initiation in polycrystalline nickel. This system was selected because it forms the basis for many superalloys used in high-temperature applications. Furthermore, prior research on this system by Grummon *et al.* [7] provided a fundamental insight on the influence of Ni–Al surface microalloys on the precursors of fatigue crack initiation. The effect of nickel self-implantation was also investigated to separate the contributions to fatigue resistance due to ion-induced lattice damage and aluminum micro-alloying.

*Paper presented at the Sixth International Conference on Surface Modification of Metals by Ion Beams, Riva del Garda, Italy, September 12–16, 1988.

0921-5093/89/$3.50

2. Experimental procedures

2.1. Specimen preparation

Cantilever beam fatigue specimens (design similar to ASTM D-671) were fabricated from an Ni-200 (99.0% Ni) sheet 1 mm thick. The gauge section was tapered to produce a constant surface stress over the gauge section area of 1.95 cm^2. Specimens were mechanically polished through 600 grit SiC paper and then annealed in an Ar–3%H_2 atmosphere for 4 h at 1073 K. This heat treatment produced a grain size with an average linear intercept of 70 μm. The gauge sections were then electropolished in a solution of 20% perchloric acid and ethanol at 230 K. In order to ensure identical thicknesses, all specimens were electropolished until a thickness of 0.94 mm was attained.

2.2. Ion beam surface modifications

The first type of modification, formation of an Ni–75at.%Al surface, was accomplished by ion beam mixing Ni–Al multilayers. Three nickel and two aluminum layers were alternately electron-beam-evaporated onto the nickel specimens producing an overall composition of Ni–75%Al in the deposited region which was 1000 Å thick. Ion beam mixing of the layers was accomplished at room temperature using 3 MeV Ni^{2+} ions generated in a 1.7 MV tandem ion accelerator. The specimens were irradiated to a fluence of 1×10^{16} ions cm^{-2}.

The second type of modification was elevated-temperature implantation of aluminum into nickel. The specimens were irradiated with 350 keV Al^+ ions to a fluence of 5×10^{17} ions cm^{-2} in a 400 kV Varian ion implanter. The ion beam current density of about 3 μA cm^{-2} was sufficient to maintain the temperature of the specimens at 723 K during implantation.

The third type of modification consisted of self-implantation of the nickel specimens with 350 keV Ni^+ ions to a dose of 1×10^{16} ions cm^{-2}. Ion beam heating resulted in a specimen temperature of about 500 K during implantation.

The modifications were applied to both sides of the fatigue specimens. In addition, the modifications (with the exception of the nickel self-implantation) were made on nickel disks 3 mm in diameter for subsequent Rutherford backscattering spectrometry (RBS) and transmission electron microscopy (TEM) analyses. The disks were thinned for TEM analysis by first protecting the modified surface with a coating of protective lacquer and then back-thinning from the unmodified side using the same electrolyte as was used for electropolishing. Several fatigue specimens that were cycled to failure were also prepared for TEM analysis using this same back-thinning procedure.

2.3. Fatigue testing

Flexural fatigue testing was accomplished on a cantilever beam testing apparatus at a frequency of 30 Hz. Strain gauges were applied to the gauge section of one specimen and the maximum bending deflection was adjusted to produce a total strain of ± 0.0012 at the surface. The fatigue tests were continued until specimen failure with periodic interruptions to extract acetate replicas from the gauge sections. The replicas were shadowed with Au–40%Pd at an angle of 30° and analyzed using optical microscopy to determine the evolution of surface fatigue damage. Surface PSB length L_A per unit area was computed from the replicas by counting the number N_L of PSB intersections per unit length of test line using the relationship [8]

$$L_A = N_L \, \pi/2$$

3. Results and discussion

3.1. Characterization of modified surfaces

Ion beam mixing of the Ni–Al multilayers produced an amorphous structure similar to previous findings [9, 10]. RBS analysis of the unmixed layers verified the overall composition of the deposited region as Ni–75%Al, and an RBS spectrum obtained after ion beam mixing indicated complete mixing of the nickel and aluminum layers. The total thickness of the amorphous layer was 1000 Å. The TEM micrograph in Fig. 1 shows a featureless microstructure and the accompanying diffraction pattern shows the diffuse rings which are characteristic of an amorphous structure.

Elevated temperature implantation of aluminum into nickel resulted in the microstructure pictured in Fig. 2(a). Figure 2(b) shows the corresponding diffraction pattern from this microstructure. Superlattice reflections corresponding to {110} planes are readily apparent, indicating the presence of the γ'-phase in the implanted region. This microstructure is similar to that reported by Ahmed and Potter [11] for elevated

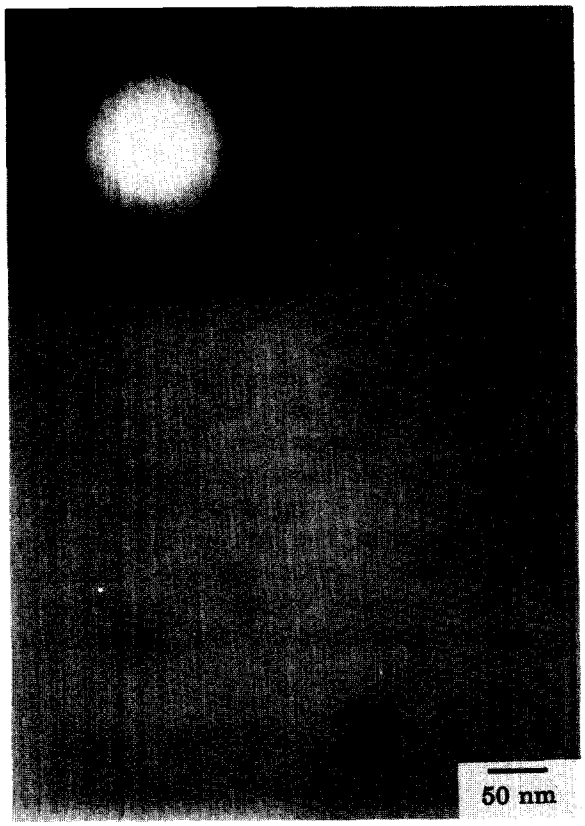

Fig. 1. Bright-field TEM micrograph showing amorphous structure resulting from room-temperature ion beam mixing of Ni–Al multilayers on nickel with 3 MeV Ni^{2+} to a fluence of 1×10^{16} ions cm^{-2}. The inset shows the diffraction pattern from the area imaged.

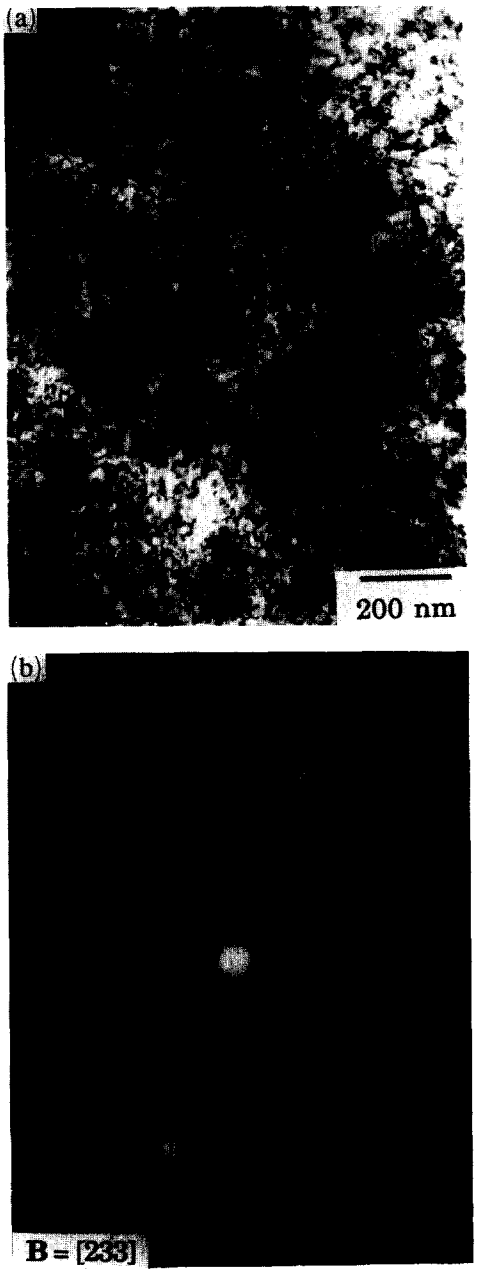

Fig. 2. (a) Bright field TEM micrograph of microstructure observed at the surface on nickel specimens implanted with 350 keV Al^+ to a fluence of 5×10^{17} ions cm^{-2} at 723 K. (b) Corresponding diffraction pattern, $B = [233]$, of area shown in (a). Superlattice spots indicate the presence of γ'.

temperature implantation of aluminum into nickel under conditions similar to those used in this study. They found that the implanted region contained γ' as well as numerous dislocation loops and other complex dislocation networks.

Although not directly investigated in this study, prior work [12] indicated that self-implantation produced point defects such as vacancies and interstitials which coalesced to form complex dislocation loop structures on {111} planes.

3.2. Evolution of surface persistent slip band structures

The effects of the surface modifications on the evolution of surface PSB features are shown in Fig. 3. Self-implantation of nickel produced a slightly lower value of L_A than the unmodified specimen. Micro-alloying the nickel surface with aluminum, whether by ion beam mixing deposited aluminum layers or direct aluminum implantation, significantly reduced the accumulation of PSB surface damage. The ion-beam-mixed Ni–75%Al modification reduced L_A by a factor of five, and the elevated-temperature aluminum implantation almost completely eliminated the formation of surface PSB features. Optical micrographs of the fatigue specimens depicting typical surface damage are shown in Fig. 4. It is impor-

tant to note that only slip bands that penetrated the surface layer were analyzed in this study. Other research [13] indicates that even though slip band features do not penetrate the surface,

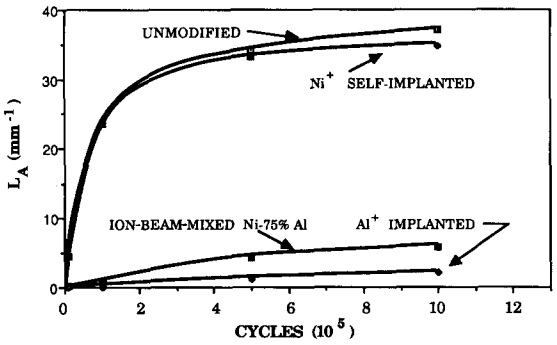

Fig. 3. Effect of surface modification on the evolution of surface slip band features. Slip band length L_A per unit area was measured on replicas extracted from fatigue specimens at various intervals during the test.

PSBs are still active just below the modified surface layer.

These results agree with those of Grummon *et al.* [14] who concluded that the increased elastic limit of the micro-alloyed Ni–Al surface region was primarily responsible for inhibiting the penetration of PSBs to the surface. They attributed the increased elastic limit to an increase in the yield strength by solid solution and precipitate strengthening and a decrease in the elastic modulus of the surface region.

TEM analysis of the aluminum-implanted and unmodified specimens after fatigue failure indicated distinctly different deformation mechanisms operating in the near-surface regions. Figure 5(a) shows the surface structure of the aluminum-implanted specimen. The structure appears similar to that observed prior to fatigue testing (see Fig. 2). The dislocation structure at the surface of the unmodified specimen (Fig. 5(b)) indicates the

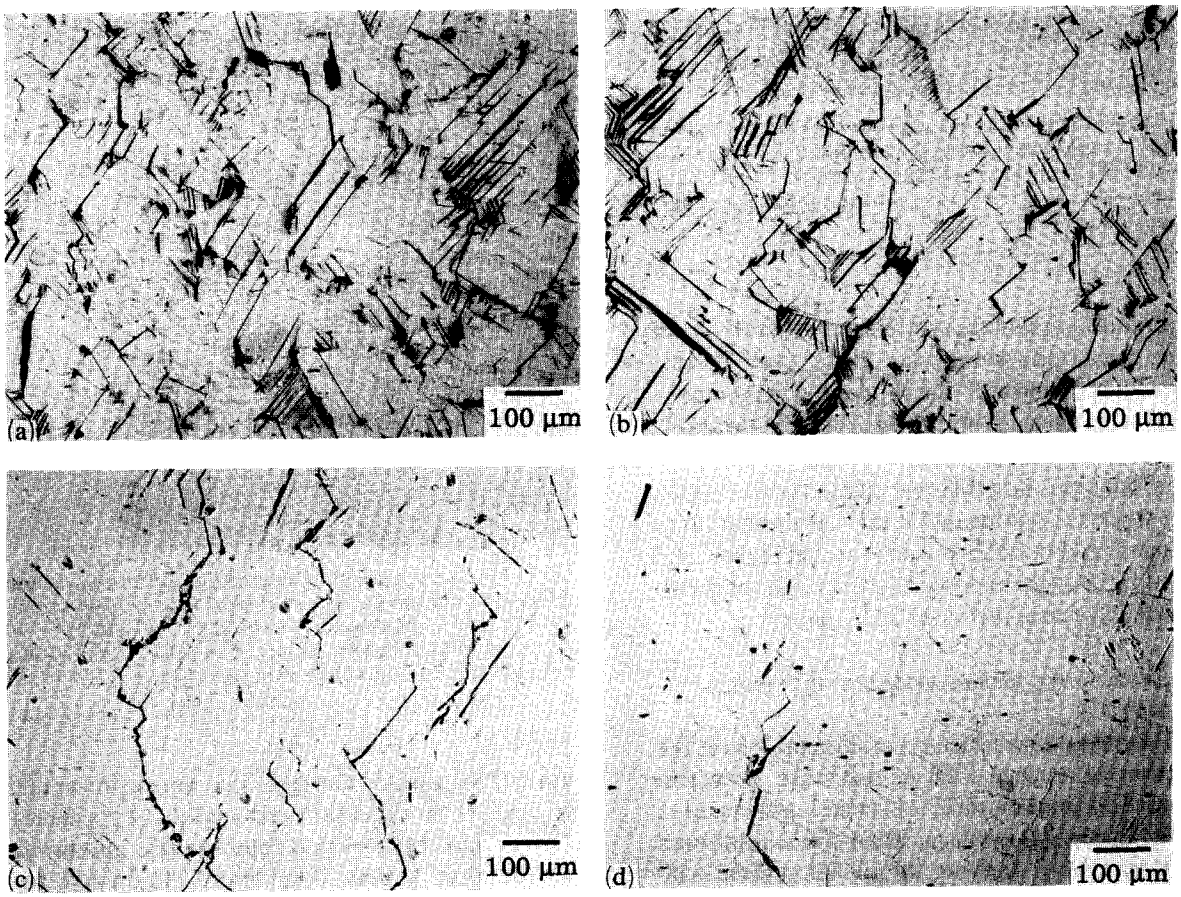

Fig. 4. Optical micrographs of fatigue specimens showing fatigue damage in (a) unmodified nickel specimen after 1 580 000 cycles, (b) 350 keV Ni^+ self-implanted specimen after 1 230 000 cycles, (c) ion-beam-mixed Ni–75%Al specimen after 1 080 000 cycles and (d) 350 keV Al^+-implanted specimen after 1 780 000 cycles.

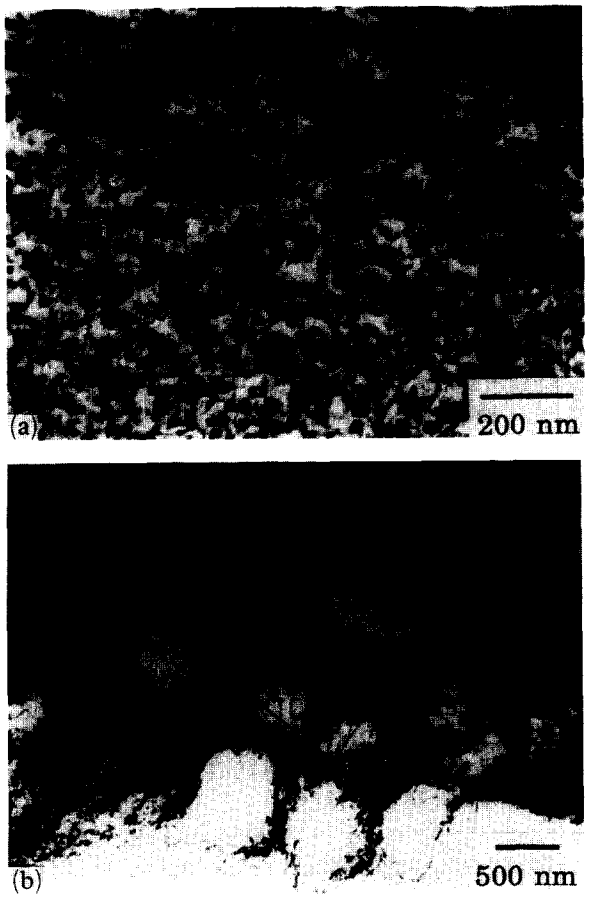

Fig. 5. Bright-field TEM micrographs showing the surface structure in (a) 350 keV Al^+-implanted specimen after 1 780 000 cycles, and (b) unmodified specimen after 1 580 000 cycles. For both micrographs $B=[\bar{1}12]$ and $g=1\bar{1}1$ (shown with arrow).

typical dislocation cell structure that is expected in fatigued f.c.c. metals [2].

Ion implantation produced a significant increase in surface hardness. Results of nano-indentation hardness tests are shown in Fig. 6. In this figure, hardness values are normalized to the unmodified specimen, *i.e.* normalized hardness H_n is the hardness of the surface modified specimen divided by the hardness of the unmodified specimen. The ion-beam-mixed Ni–75%Al surface more than doubled the near-surface hardness and the aluminum implantation and nickel self-implantation produced a smaller hardness increase. The fact that the self-implantation and aluminum implantation produced a similar hardness increase indicated that a significant portion of the hardness increase was due to lattice defects produced during the implantation process. The higher hardness in the ion-beam-mixed Ni–

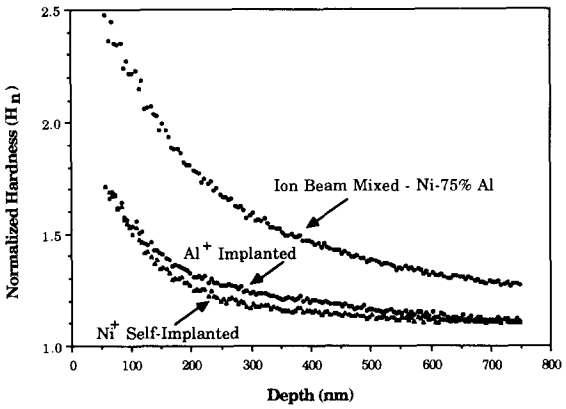

Fig. 6. Hardness–depth profiles of the near surface regions of ion-beam-modified nickel. Normalized hardness H_n is the hardness of the modified specimen divided by the hardness of the unmodified specimen at the same depth.

75%Al specimen was probably due to the higher implantation energy (3 MeV *vs.* 350 keV) and the amorphous structure of the near-surface region.

These results indicate that surface hardness may not be a dominant factor in the suppression of surface PSB features. The nickel self-implantation produced a significant increase in surface hardness but very little suppression of PSB features. It is possible that the lattice defect structure induced by self-implantation is transformed to a more stable state by dislocation interactions generated during fatigue cycling, while the hardening effect of aluminum (through solid solution and precipitate hardening) is able to maintain its strengthening character and resist the emergence of mobile dislocations from the interior to the surface, thus inhibiting the appearance of surface PSB features. Detailed TEM studies of the near-surface regions of fatigued and unfatigued specimens are being conducted to clarify this issue.

3.3. Fatigue crack initiation and growth

Micrographs depicting early stages of fatigue crack initiation are shown in Fig. 7. The self-implanted and unmodified specimens formed microcracks along slip bands after only 10 000 cycles. Figure 7(a) is an optical micrograph of a replica of the self-implanted specimen taken after 10 000 cycles that shows a crack initiating at a PSB that traverses the entire grain. In self-implanted and unmodified specimens, cracks preferentially formed at narrow PSBs rather than at the wider bands and propagated across the width of the specimens primarily by a linking of

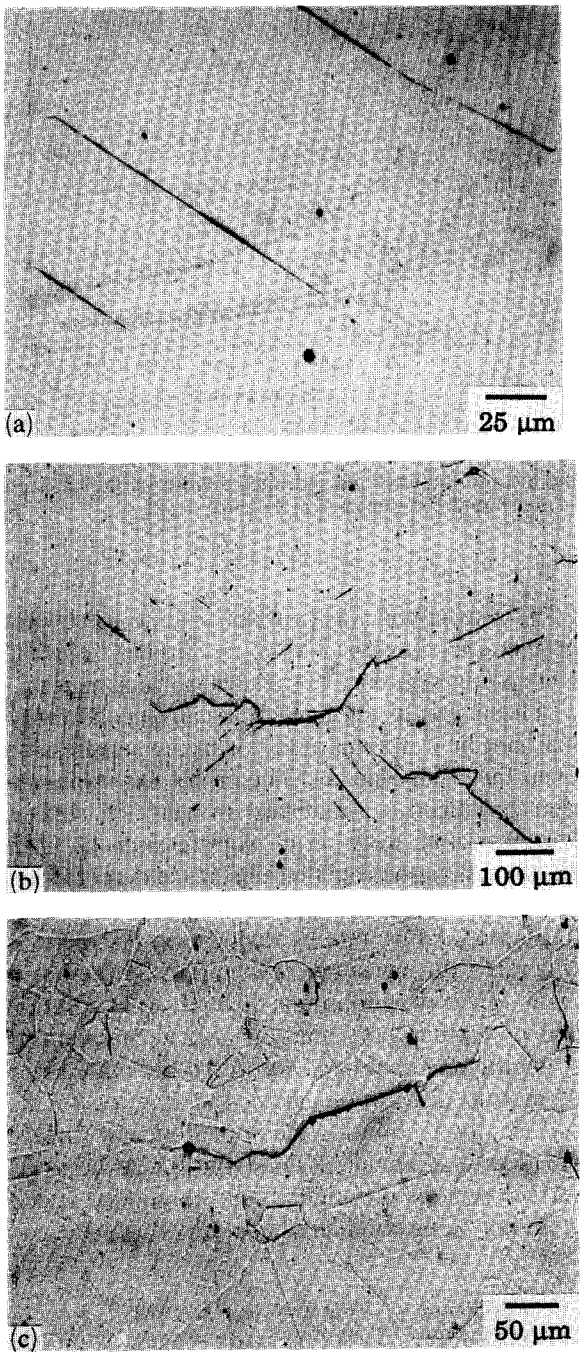

Fig. 7. Optical micrographs of surface replicas showing typical crack initiation modes in (a) 350 keV Ni^+ self-implanted specimen after 10 000 cycles, (b) ion-beam-mixed Ni–75%Al specimen after 500 000 cycles and (c) 350 keV Al^+-implanted specimen after 500 000 cycles.

slip band cracks with occasional linking occurring along grain boundaries.

Crack initiation was significantly delayed in both types of specimens that were micro-alloyed with aluminum. In the ion-beam-mixed Ni–75%Al and aluminum-implanted specimens, fatigue cracks were first detected in the replicas taken after 500 000 cycles. Figure 7(b) shows the intergranular crack initiation mode in the specimen with the ion-beam-mixed Ni–75%Al surface modification. In this specimen, crack propagation occurred primarily along grain boundaries. In the aluminum-implanted specimen, cracks initiated primarily at grain boundaries, although a significant amount of slip band crack initiation was also observed. Transgranular and intergranular crack propagation was evident in the aluminum-implanted specimen.

TABLE 1 Cycles to failure

Surface condition	*Cycles to failure*
Unmodified	1 580 000
Nickel self-implantation	1 230 000
Ion-beam-mixed Ni–75%Al	1 080 000
Aluminum implanted	1 780 000

The change in crack initiation mode from PSBs to grain boundaries has been observed in other studies [15–18]. The shift to intergranular crack initiation was usually accompanied by significant suppression of PSB penetration to the surface. This observation led Hohmuth *et al.* [15] to propose that compatibility stresses generated at grain boundaries are reduced by slip band formation. Blocking the penetration of these slip bands to the surface results in higher compatibility stresses which promote intergranular cracking. Another possible explanation is based on the observation that intergranular cracks can initiate where PSBs impinge on the grain boundary [19]. Suppressing the penetration of PSBs to the surface may cause the impingement stresses to increase and result in a greater susceptibility for intergranular crack initiation.

Although crack initiation was delayed in specimens that were surface micro-alloyed with aluminum, no consistent effect on fatigue life was observed. Cycles to failure for the different surface conditions are given in Table 1.

The small number of specimens tested and the fact that some specimens initiated cracks at the edges prevented meaningful determination of the influence of ion micro-alloying on fatigue life.

4. Conclusions

The results of the study indicated that micro-alloying the surfaces of nickel fatigue specimens

with aluminum by ion beam mixing evaporated nickel and aluminum multilayers or elevated-temperature aluminum implantation increased surface hardness and significantly inhibited the formation of surface PSB features. In addition, the aluminum caused a shift in crack initiation mode from transgranular to intergranular. Lattice defects induced during the implantation process increased the surface hardness but did not suppress the formation of surface PSB features.

Acknowledgments

We gratefully acknowledge the National Science Foundation for support of this work under Grant DMR 8603174 and the use of the facilities at the Michigan Ion Beam Laboratory for Surface Modification and Analysis at the University of Michigan.

References

1 N. Thompson, N. Wadsworth and N. Louat, *Philos. Mag., 1* (1956) 113–126.
2 H. Mughrabi, in G. C. Sih and J. W. Provan (eds.), *Defects, Fracture, and Fatigue, Proc. Second Int. Symp. on Defects, Fracture, and Fatigue, Mont Gabriel, Canada*, The Hague, Martinus Nijhoff, 1983, pp. 15–28.
3 R. G. Vardiman, in R. F. Hochman (ed.), *Proc. Conf. on Ion Plating and Implantation Applications to Materials, Atlanta, GA*, American Society for Metals, Metals Park, OH, 1986, pp. 107–113.
4 E. Y. Chen and E. A. Starke, *Mater. Sci. Eng., 24* (1976) 209–221.
5 A. Kujore, S. B. Chakrabortty, E. A. Starke and K. O. Legg, *Nucl. Instrum. Methods, 182/183* (1981) 949–958.
6 J. G. Han and R. F. Hochman, *Mater. Sci. Eng., 90* (1987) 317–325.
7 D. S. Grummon, J. W. Jones, J. M. Eridon, G. S. Was and L. E. Rehn, *Nucl. Instrum. Methods B, 19/20* (1987) 227–231.
8 F. N. Rhines, *Fatigue Mechanisms, Proc. ASTM-NBS-NSF Symp. ASTM Spec. Tech. Publ., 675* (1979) 23–46.
9 G. S. Was and J. M. Eridon, *Nucl. Instrum. Methods B, 24/25* (1987) 557–561.
10 M. Nastasi, J. M. Williams, E. A. Kenik and J. W. Mayer, *Nucl. Instrum. Methods B, 19/20* (1987) 543–548.
11 M. Ahmed and D. I. Potter, *Acta Metall., 35(9)* (1987) 2341–2354.
12 B. O. Hall and D. I. Potter, *Effects of Irradiation on Structural Materials, ASTM Spec. Tech. Publ., 683* (1979) 32–45.
13 D. S. Grummon, D. J. Morrison, J. W. Jones and G. S. Was, *Mater. Sci. Eng., A114* (1989).
14 D. S. Grummon, J. W. Jones and G. S. Was, *Metall. Trans. A, 19* (1988) 2775.
15 K. Hohmuth, E. Richter, B. Rauschenbach and C. Blochwitz, *Mater. Sci. Eng., 69* (1985) 191–201.
16 A. W. Sleeswyk, H. J. G. Kok and G. Boom. *Scr. Metall., 14* (1980) 919–922.
17 K. V. Jata, J. G. Han, E. A. Starke and K. O. Legg, *Scr. Metall., 17* (1983) 479–483.
18 R. G. Vardiman and J. E. Cox, *Acta Metall., 33(11)* (1985) 2033–2039.
19 H. Mughrabi, in G. C. Sih and J. W. Provan (eds.), *Defects, Fracture, and Fatigue, Proc. Second Int. Symp. on Defects, Fracture, and Fatigue, Mont Gabriel, Canada*, Martinus Nijhoff, The Hague, 1983, pp. 139–146.